# Identification of a Pyroptosis-Related lncRNA Risk Model for Predicting Prognosis and Immune Response in Colon Adenocarcinoma

**Yuying Tan**
Central South University
**Liqing Lu**
Central South University
**Xujun Liang**
Central South University
**Yongheng Chen** ( yonghenc@163.com )
Central South University

**Research Article**

**Keywords:** colon adenocarcinoma, ceRNA network, pyroptosis, tumor immune microenvironment, immunotherapy

**Posted Date:** January 11th, 2022

**DOI:** https://doi.org/10.21203/rs.3.rs-1234682/v1



**Version of Record:** A version of this preprint was published at World Journal of Surgical Oncology on April 12th, 2022. See the published version at https://doi.org/10.1186/s12957-022-02572-8.

# Abstract

**Background:** Colon adenocarcinoma (COAD) is one of the most common malignant tumors and diagnosed at an advanced stage with poor prognosis in the world. Pyroptosis is involved in the initiation and progression of tumors. This research focused on constructing a pyroptosis-related ceRNA network to generate a reliable risk model for risk prediction and immune infiltration analysis of COAD.

**Methods:** Transcriptome data, miRNA-sequencing data and clinical information were downloaded from the TCGA database. Firstly, differentially expressed mRNAs (DEmRNAs), miRNAs (DEmiRNAs), and lncRNAs (DElncRNAs) were identified to construct a pyroptosis-related ceRNA network. Secondly, a pyroptosis-related lncRNA risk model was developed applying univariate Cox regression analysis and least absolute shrinkage and selection operator method (LASSO) regression analysis. The Kyoto Encyclopedia of Genes and Genomes (KEGG) and Gene Ontology (GO) enrichment analyses were utilized to functionally annotate RNAs contained in the ceRNA network. In addition, Kaplan-Meier analysis, receiver operating characteristic (ROC) curves, univariate and multivariate Cox regression, and nomogram were applied to validate this risk model. Finally, the relationship of this risk model with immune cells and immune checkpoint blockade (ICB) related genes were analyzed.

**Results**: Totally 5373 DEmRNAs, 1159 DElncRNAs and 355 DEmiRNAs were identified. A pyroptosis-related ceRNA regulatory network containing 132 lncRNAs, 7miRNAs and 5 mRNAs was constructed and a ceRNA-based pyroptosis-related risk model including 11 lncRNAs was built. Tumor tissues were classified into high- and low- risk groups according to the median risk score. Kaplan-Meier analysis showed that the high-risk group had a shorter survival time; ROC analysis, independent prognostic analysis and nomogram further indicated the risk model was a significant independent prognostic factor which had excellent ability to predict patients' risk. Moreover, immune infiltration analysis indicated that the risk model was related to immune infiltration cells (i.e., B cells naïve, T cells follicular helper, Macrophages M1, etc.) and ICB-related genes (i.e., *PD-1*, *CTLA4*, *HAVCR2*, etc).

**Conclusions:** This pyroptosis-related lncRNA risk model possessed good prognostic value and the ability to predict the outcome of ICB immunotherapy in COAD.


# Introduction

Colorectal cancer (CRC) is the most common cancer diagnosed in the world [1]. The incidence and mortality rates of CRC are in the top three of all cancers based on the American Cancer Society 2021 report [1]. Colon adenocarcinoma (COAD) is the most common histological subtype of CRC. With the advancement in the diagnosis and treatment of COAD in recent years, its incidence and mortality remain at 10.2% and 9.2%, respectively[2]. Therefore, the improvement of early diagnosis and treatment modalities for COAD patients is an urgent clinical need.

Pyroptosis is a gasdermin-mediated inflammatory programmed cell death characterized by cell swelling, pore formation and the release of intracellular contents, such as IL-1β and IL-18 [3]. Pyroptosis is typically

triggered by canonical pathways and non-canonical pathways [4, 5]. In the past several years, increasingly studies have depicted that pyroptosis was involved in the progress of cancer. The primary therapeutic strategy of cancer is to induce cell death, and some researchers are trying to find novel targeted therapies for COAD by activating the pyroptosis pathways [6].

The competitive Endogenous RNA (ceRNA) hypothesis, including non-coding RNAs and mRNAs, is considered as a novel regulatory network, which reveals a novel mechanism of interaction between RNAs. These ceRNA molecules can compete to bind the same miRNA through MicroRNA Response Elements (MRE) to affect the gene expression [7]. Long non-coding RNA (lncRNA), more than 200 nucleotides in length, is defined as a non-coding RNA and has been found to be involved in diverse key biological processes, including cell proliferation and differentiation, genetic regulation of gene expression, and regulation of microRNAs (miRNAs) [8]. Studies have shown that lncRNAs can disrupt the balance of the ceRNA network, thereby promoting cancer progression. [9, 10]. For example, Yeshuo Ma et al. depicted that the lncRNA RP1-85F18.6 was upregulated in CRC and played major roles in tumorigenesis and repressed the pyroptosis of CRC cells [11]. In addition, several studies described that lncRNAs promote tumorigenesis by changing the immune microenvironment in cancers [12, 13]. To date, the pyroptosis-related ceRNA networks have not been elucidated for COAD.

In this study, transcriptome and miRNA sequencing data between COAD tumor tissues and normal tissues were retrieved from The Cancer Genome Atlas (TCGA) database. The pyroptosis-related ceRNA network was constructed using integrated analysis. A pyroptosis-related prognostic signature was extracted from the ceRNA network. Then, we investigated the role of this pyroptosis-related lncRNAs prognostic signature in immune microenvironment and immune checkpoint inhibitor treatment.

## Materials And Methods

# Data Acquisition

RNA-sequencing data were derived from the TCGA database about COAD including 398 tumor samples and 39 normal samples. The miRNA-sequencing data were downloaded from the TCGA database including 380 tumor samples and 8 normal samples. Meanwhile, relevant clinical data of 385 COAD patients were also obtained from TCGA, including age, gender, survival status, stage, T, N, and M classification (Table 1).

# Identification of Differentially Expressed Genes (DEGs)

The R package “edgeR” was applied to identify the DEGs of lncRNA, mRNA,and miRNAs with false discovery rate (FDR) adjusted $P<0.05$ and $|log2FC|>1.0$ as the cut-off criterion. Then, the volcano maps and heatmaps were plotted employing “ggplot2” and “pheatmap” R packages.

# Construction of a Pyroptosis-Related ceRNA Network

The miRcode database was applied to predict the interaction pairs between lncRNAs and miRNAs [14]. The DEmiRNAs targeted DEmRNAs (miTGs) were obtained from TargetScan, miRTarBase, and miRDB databases [15, 16]. In addition, the pyroptosis-related DEmRNAs were retrieved by the intersection of miTGs, DEmRNAs and 155 pyroptosis-related genes (PRGs) from geneCards (https://www.genecards.org/, Supplement Table S1). Finally, a pyroptosis-related ceRNA network was visualized using Cytoscape v3.8.2.

# Identification and Validation of a ceRNA Based Pyroptosis-Related lncRNA Risk Model

379 COAD patients with survival data were included. 132 pyroptosis-related lncRNAs (PRlncRNAs) in the above ceRNA network were analyzed by univariate Cox regression analysis to filtrate PRlncRNAs associated with survival. To avoid overfitting, PRlncRNAs were screened via least absolute shrinkage and selection operator (LASSO) regression analysis (R package “glmnet”, $p<0.05$). Then, a pyroptosis-related lncRNA risk model was constructed and the risk score of each sample was calculated based on the formula below:

$$\text{Risk Score} = \sum_i \text{Xi} \times \text{Yi}$$

(X: coefficients, Y: lncRNA expression level). And tumor tissues were separated into high- and low-risk groups according to the median risk score. Next, lncRNAs in the PRlncRNA risk model with associated DEmiRNAs and DEmRNAs were used to construct a prognostic ceRNA network and to conduct Gene Ontology (GO) and Kyoto Encyclopedia of Genes and Genomes (KEGG) functional enrichment analyses (R packages “clusterProfiler”, “org.Hs.eg.db” and “enrichplot”).

# Validation of the Risk Model

Kaplan-Meier analysis was used to compare the overall survival (OS) time between the two risk groups using R packages “survival” and “survminer”. The 1-, 3- and 5-year receiver operating characteristic (ROC) curves were acquired by utilizing “timeROC”, “survival” and “survminer” R packages. Independent prognostic analysis showed the relationship of risk score and clinical traits through the “survival”, “survminer” and “forestplot” R packages.

# Establishment of The Nomogram

A nomogram was established to quantitatively calculate patients' survival. Then, calibration curves were employed to confirm the predictive effect of nomogram. (R package "rms").

## Immune Cells Infiltration and Immune Checkpoint Blockades (ICBs) Analysis

The relationship between the immune cell proportion and risk score was estimated by the CIBERSORT algorithm ($p<0.05$). Spearman correlation analysis was employed to estimate the association of the immune cells and risk score.

The expression level of ICB-related genes was closely involved with the outcome of immunotherapy. Therefore, the Spearman correlation between the 11 ICB-related genes and risk score were analyzed [17].

## Statistical Analysis

All statistical analyses used Perl v5.32.1 and R 4.1.0 software. The ceRNA network was constructed by Cytoscape v3.8.2. Wilcox test was used to compare the proportion of immune cells between the two groups. DEmRNAs, DElncRNAs and DEmiRNAs were gained with the threshold as FDR <0.05 and |log2Fold Change|>1. Statistical tests were two-tailed ($p<0.05$).

# Results

## DEmRNAs, DElncRNAs and DEmiRNAs

The flow diagram of the current study is shown in Figure 1.

A total of 5373 DEmRNAs (2886 upregulated and 2487 downregulated), 355 DEmiRNAs (217 upregulated and 138 downregulated) and 1159 DElncRNAs (819 upregulated and 340 downregulated) were obtained through comparing COAD and normal tissues in TCGA-COAD database. The volcano maps and heatmaps showed the DEmRNAs, DEmiRNAs and DElncRNAs expression of COAD respectively. (Figures 2A-F).

## Construction of a Pyroptosis-Related ceRNA Network in COAD

To construct the pyroptosis-related ceRNA network, several databases were used. Based on the miRcode database, the lncRNA-miRNA interactions including 218 DElncRNAs and 38 DEmiRNA were identified. The

interaction of miRNA-mRNA including 38 miRNAs and 1533 miTGs was acquired based on TargetScan, mirTarBase and miRDB databases. Then, we screened out 5 pyroptosis-related genes by taking the intersection of 1533 miTGs, 5373 DEmRNAs and 155 pyroptosis-related genes (Figure 3A). Finally, 5 DEmRNAs, 7 DEmiRNAs and 132 DElncRNAs were gained, then we constructed a pyroptosis-related network of COAD. (Figure 3B, Supplement Table S2).

# Construction of a PRlncRNA Prognostic Risk model

We screened 11 survival-related lncRNAs by employing univariate Cox regression analysis ($p<0.05$, Supplement Table S3). Among them, 8 lncRNAs (*HOTAIR*, *LINC00402*, *SFTA1P*, *LINC00461*, *DSCR8*, *CYP1B1-AS1*, *LINC00330*, *ALMS1-IT1*) were risk genes with HR>1 and other 3 lncRNAs (*ZRANB2-AS1*, *MYB-AS1*, *TP53TG1*) were protective genes with HR<1 (Figure 4A, Table 2). Subsequently, the 11 lncRNAs were incorporated into LASSO regression analysis to avoid overfitting, and a prognostic PRlncRNA risk model was constructed including the above 11 lncRNAs (Figures 4B, C). The risk score was computed as the following formula: risk score = (0.0013***HOTAIR* exp) + (0.0174***LINC00402* exp) + (0.0186***SFTA1P* exp) + (0.0373***LINC00461* exp) + (-0.2108***ZRANB2*-AS1 exp) + (-0.0012** *TP53TG1* exp) + (-0.0647** *MYB-AS1* exp) + (0.0032** *DSCR8* exp) + (0.0084** *LINC00330* exp) + (0.0156** *CYP1B1-AS1* exp) + (0.0053***ALMS1-IT1* exp). COAD patient was categorized into high or low risk groups in terms of median risk value. According to the previous ceRNA hypothesis, 7 miRNA (*hsa-mir-155*, *hsa-mir-21*, *hsa-mir-182*, *hsa-mir-96*, *hsa-mir-152*, *hsa-mir-17*, *hsa-mir-106a*) and 5 mRNAs (*CEBPB*, *IL1B*, *SESN2*, *ALK*, *TXNIP*) were obtained, and then we re-established a ceRNA network based on them (Figure 4D).

# Functional Enrichment Analysis of the Pyroptosis-Related ceRNA Genes

To explore potential functions of these 11 lncRNAs, 7miRNAs and 5mRNAs in biological processes, GO and KEGG function enrichment analyses were performed with P value < 0.05 as the threshold. For GO analysis, these genes were primarily enriched in the cellular response to biotic stimulus and lipid catabolic process in biological processes (BPs); TORC2 complex, GATOR2 complex and TOR complex in cellular components (CCs); ubiquitin-like protein ligase binding in molecular function (MF) (Figure 4E). KEGG pathway analysis suggested these genes were markedly concentrated in the IL-17 signaling pathway, TNF signaling pathway, Tuberculosis, and NOD-like receptor signaling pathway (Figure 4F).

# Validation of PRlncRNA Prognostic Risk Model

In the prognostic PRlncRNA risk model, 8 lncRNAs (*HOTAIR*, *LINC00402*, *SFTA1P*, *LINC00461*, *DSCR8*, *CYP1B1-AS1*, *LINC00330*, *ALMS1-IT1*) were upregulated while other 3 lncRNAs (*ZRANB2-AS1*, *MYB-AS1*, *TP53TG1*) were downregulated in tumor tissues (Figure 5A). Kaplan-Meier analysis showed that patients in the high-risk group had shorter survival times (Figure 5B). Likewise, patients were separated into two

risk groups based on the median risk score (Figure 5C). As the risk score increased, the patient's survival time decreased gradually (Figure 5D). ROC analysis indicated that the PRlncRNA risk model was able to excellently predict the 1-year (0.744), 3-year (0.696) and 5-year (0.623) survival of COAD patients, respectively (Figure 5E).

# Independent Prognostic Analysis of the Prognostic PRlncRNA Risk Model

To explore whether the prognostic PRlncRNA risk model can be an independent prognostic factor, univariate and multivariate Cox regression analyses were employed. The univariate Cox regression analysis showed that the hazard ratio (HR) of this risk model was 3.054 (95% CI: 2.185-4.269) (Figure 6A). And we got consistent results using the multivariate Cox model (HR: 2.647, 95%CI:1.841-3.804) (Figure 6B). Eventually, these results implied that our prognostic PRlncRNA risk model can be an independent prognostic factor independent of other clinical characteristics. Moreover, the heatmap of clinical characteristics implied that the survival status of patients was differentially distributed between low- and high-risk subgroups ($p<0.05$, Figure 6C).

# Construction of a Predictive Nomogram

To further assess whether this prognostic PRlncRNA risk model had optimal predictive capabilities, we collected clinical characteristics, including age, gender and stage, as the candidate predictive biomolecular indicators. We constructed a nomogram with risk, age, gender and stage (Figure 7A). The calibration curves suggested that the nomogram had good predictive power (Figures 7B-D). The above findings showed a promising capacity of the PRlncRNA risk model for patient prognosis and survival prediction.

# Immunoinfiltration Analysis

Pyroptosis plays an important role in regulating the tumor-immune microenvironment (TIME). In the current study, the CIBERSOR algorithm was utilized to investigate the relevance of risk scores to immune infiltrating cells (Figure 8A). B cells naïve, T cells CD8, T cells follicular helper, T cells regulatory (Tregs) and Macrophages M1 were higher expressed while T cells CD4 memory resting, Dendritic cells activated and Mast cells activated were lower expressed in the high-risk group by using Wilcoxon rank-sum test (Fig 8B). Additionally, we performed correlation analysis between prognostic risk model with the above eight significant difference immune infiltrating cells, and the results showed that the risk score positively related to the immune infiltration of B cells naïve (R=0.19, p=2e-04), Macrophages M1 (R=0.17, p=0.0012), T cells CD8 (R=0.21, p=4.7e-05) and T cells follicular helper (R=0.13, p=0.011), while negatively associated with T cells CD4 memory resting infiltration (R=-0.19, p=0.00015) (Figure 8C).

# Relationship of the Prognostic PRlncRNA Risk Model and Immune Checkpoint Blockades (ICBs)

ICB-related immunotherapy had become a promising modality for patients with COAD. To investigate the response of COAD samples to immunotherapy, we examined the association of ICB-related genes (i.e., *PD-1*, *CTLA4*, *HAVCR2*, etc) and risk score (Figure 9A). The results showed that risk score was significantly positively correlated with *PD-1* (R=0.245, p=1.44e-06), *PD-L1* (R=0.24,P=2.5e-06), *PD-L2* (R=0.15, p=0.0025), *GITR* (R=0.13,p=0.012), *HAVCR2* (R=0.17,p=0.00065) and *CTLA4* (R=0.18, p=0.00044), while negatively associated with *SOAT1* (R=-0.1, p=0.042), indicating that risk score model was useful in assessing patients' response to immunotherapy (Figure 9B).

## Discussion

Colon adenocarcinoma (COAD) is the most common malignancy with increased mortality in the world [18]. Despite significant improvements in surgery, radiotherapy, chemotherapy, and immunotherapy, the rates of 5-year survival remain low [19]. Therefore, it is crucial to identify potential biomarkers for the diagnosis and treatment of COAD. Pyroptosis was regarded as a new type of programmed cell death that played a dual function in the development of cancer [3]. In recent years, pyroptosis has become a hot topic in the field of oncology research, and more and more researches have emphasized the key effects of pyroptosis in tumorigenesis and TIME [20-22]. ceRNA represents a new regulation mode of gene expression, which is more sophisticated and complex than the miRNA regulatory network. There are growing evidences that the ceRNA network is involved in the progression of COAD. [23, 24]. Nevertheless, the underlying function of ceRNA based pyroptosis-related risk model in prognostic prediction and tumor immunity of COAD has not yet been elucidated, and our study was designed to clarify this role.

Our study constructed a pyroptosis-related ceRNA network and PRlncRNA risk model. Moreover, we also explored the prognosis predictive ability of the risk model and its association with immune cells infiltration, and assessed the reactivity of COAD patients to ICB therapy.

In current research, a pyroptosis-related ceRNA regulatory network including 5 mRNAs, 7 miRNAs and 11 lncRNAs was firstly constructed to investigate the potential molecular mechanism of the ceRNA network. Furthermore, GO and KEGG enrichment analysis showed that these genes were mostly enriched in the IL-17 signaling pathway and TNF signaling pathway et.al. These results suggested that this pyroptosis-related ceRNA network can be a new tool to predict clinical results of COAD. However, these discoveries need to be verified in additional studies. Moreover, 11 pyroptosis-related lncRNAs were incorporated into developing a PRlncRNA risk model. Then, Kaplan–Meier curve, time-dependent ROC curves, Cox regression analysis, and nomogram showed that this risk model possessed excellent prediction ability and became an independent predictor of COAD prognosis.

A growing body of evidences have demonstrated that lncRNAs play an essential role in regulating immune cell infiltration [25, 26], and some researches also reported that pyroptosis of tumor cells regulate

tumor-suppressed immune cells [21, 22]. Furthermore, we investigated the fundamental effects of the risk score in the regulation of TIME. Consistent with the previous reports, our research also showed that risk score was negatively correlated with resting immune cells' proportions, while positively associated with immunosuppressive cells', indicating that patients with low-risk scores were immunologically resting, while with high-risk score represents immunosuppressive tumor microenvironment.

With the development of immune checkpoint inhibitors, ICB immunotherapy has generated promising therapeutic results in COAD [27, 28]. To date, immunotherapy has become the fifth pillar in the foundation of COAD therapeutics. Unfortunately, the majority of COAD patients did not respond to ICB treatment [29]. Pyroptosis can alter the immune microenvironment and remodel immune cells to enhance the efficiency of tumor immunotherapies [30]. Previous researches have demonstrated that pyroptosis induction plus with PD-1 improves the anti-tumor activity [22, 31]. Thus, a novel PRlncRNA risk model was developed to investigate the correlation of pyroptosis and ICB-related genes, and to predict COAD patients' responses to ICB immunotherapy. The current study has shown that the PRlncRNA risk model was strongly related to ICB-related genes (i.e., PD-1, PD-L1, et al), which implied that the PRlncRNA risk model could be utilized to evaluate the response to ICB treatment of COAD patients. Meanwhile, further validation of the PRlncRNA risk model as a useful predictor of immune checkpoint therapy in COAD is needed in the future.

Our research has some limitations. All analyses were employed by using the TCGA-COAD cohort, which would be better to validate with other database cohorts. In addition, in vivo and in vitro experiments should be conducted to further verify our results. However, the novelty of our study is that for the first time, the molecular mechanism of COAD was investigated from the perspective of the pyroptosis-related ceRNA network. Additionally, 11 pyroptosis-related lncRNA prognostic biomarkers were screened based on the ceRNA network. Moreover, the PRlncRNA risk model possessed a highly predictive ability for survival in the COAD patients. This may provide a new idea for the study of COAD.

# Conclusions

To sum up, we performed comprehensive and systematic bioinformatics analysis and constructed a PRlncRNA risk model for COAD patients, which could be used as a potent tool in predicting the prognosis of COAD patients. In addition, the risk model was related to TIME and ICB-related genes. The pyroptosis-related ceRNA network might be promising therapeutic targets of COAD.

# Abbreviations

DEGs: Differentially expressed genes; FC: Fold change; FDR: False discovery rate; GO: Gene Ontology; KEGG: Kyoto Encyclopedia of Genes and Genomes; TCGA: The Cancer Genome Atlas; ROC: receiver operating characteristic; ICB: immune checkpoint blockade; LASSO: least absolute shrinkage and selection operator method; ceRNA: competitive Endogenous RNA; MRE: MicroRNA Response Elements; PRlncRNAs: pyroptosis-related lncRNAs.

## Declarations

# Acknowledgments

We appreciate laboratory members for thoughtful suggestions and comments on the manuscript.

# DATA AVAILABILITY STATEMENT

This study analyzed publicly available datasets which were obtained from the following sources: mRNA expression profile, miRNA expression profile, lncRNA expression profile and clinical information of COAD were acquired from TCGA-COAD (https://portal.gdc.cancer.gov/).

# AUTHOR CONTRIBUTIONS

Conceptualization, YT and YC; methodology, LL and YT; formal analysis, LL and YT; writing, LL and YT; review and editing, YT and XL; funding acquisition, LL and YC. All authors have read and agreed to the published version of the manuscript.

# FUNDING

This work was supported by the National Natural Science Foundation of China (grants 81570537 and 81974074 to Y.C). Graduate Innovation projects of Central South University (1053320182802 to L.L).

# CONFLICT OF INTEREST

The authors declare that the research was conducted in the absence of any commercial or financial relationships that could be construed as a potential conflict of interest.

# Ethics approval and consent to participate

Not applicable.

# Consent for publication

Not applicable

## References

1. Siegel RL, Miller KD, Fuchs HE, Jemal A: **Cancer Statistics, 2021.** *CA Cancer J Clin*2021, **71:**7-33.

2. Liu Y, Li C, Dong L, Chen X, Fan R: **Identification and verification of three key genes associated with survival and prognosis of COAD patients via integrated bioinformatics analysis.** *Biosci Rep*2020, **40**.
3. Shi J, Zhao Y, Wang K, Shi X, Wang Y, Huang H, Zhuang Y, Cai T, Wang F, Shao F: **Cleavage of GSDMD by inflammatory caspases determines pyroptotic cell death.** *Nature*2015, **526:**660-665.
4. Wu D, Wang S, Yu G, Chen X: **Cell Death Mediated by the Pyroptosis Pathway with the Aid of Nanotechnology: Prospects for Cancer Therapy.** *Angew Chem Int Ed Engl*2021, **60:**8018-8034.
5. Hsu SK, Li CY, Lin IL, Syue WJ, Chen YF, Cheng KC, Teng YN, Lin YH, Yen CH, Chiu CC: **Inflammation-related pyroptosis, a novel programmed cell death pathway, and its crosstalk with immune therapy in cancer treatment.** *Theranostics*2021, **11:**8813-8835.
6. Yu P, Zhang X, Liu N, Tang L, Peng C, Chen X: **Pyroptosis: mechanisms and diseases.** *Signal Transduct Target Ther*2021, **6:**128.
7. Salmena L, Poliseno L, Tay Y, Kats L, Pandolfi PP: **A ceRNA hypothesis: the Rosetta Stone of a hidden RNA language?** *Cell*2011, **146:**353-358.
8. Li X, Wu Z, Fu X, Han W: **Long Noncoding RNAs: Insights from Biological Features and Functions to Diseases.** *Med Res Rev*2013, **33:**517-553.
9. Peng WX, Koirala P, Mo YY: **LncRNA-mediated regulation of cell signaling in cancer.** *Oncogene*2017, **36:**5661-5667.
10. Taniue K, Akimitsu N: **The Functions and Unique Features of LncRNAs in Cancer Development and Tumorigenesis.** *Int J Mol Sci*2021, **22**.
11. Ma Y, Chen Y, Lin C, Hu G: **Biological functions and clinical significance of the newly identified long non-coding RNA RP1-85F18.6 in colorectal cancer.** *Oncol Rep*2018, **40:**2648-2658.
12. Atianand MK, Caffrey DR, Fitzgerald KA: **Immunobiology of Long Noncoding RNAs.** *Annu Rev Immunol*2017, **35:**177-198.
13. Chen YG, Satpathy AT, Chang HY: **Gene regulation in the immune system by long noncoding RNAs.** *Nat Immunol*2017, **18:**962-972.
14. Jeggari A, Marks DS, Larsson E: **miRcode: a map of putative microRNA target sites in the long non-coding transcriptome.** *Bioinformatics*2012, **28:**2062-2063.
15. Hsu SD, Lin FM, Wu WY, Liang C, Huang WC, Chan WL, Tsai WT, Chen GZ, Lee CJ, Chiu CM, et al: **miRTarBase: a database curates experimentally validated microRNA-target interactions.** *Nucleic Acids Res*2011, **39:**D163-169.
16. Wong N, Wang X: **miRDB: an online resource for microRNA target prediction and functional annotations.** *Nucleic Acids Res*2015, **43:**D146-152.
17. Chen R, Chen Y, Huang W, Zhao Y, Luo W, Lin J, Wang Z, Yang J: **Comprehensive analysis of an immune-related ceRNA network in identifying a novel lncRNA signature as a prognostic biomarker for hepatocellular carcinoma.** *Aging (Albany NY)*2021, **13:**17607-17628.
18. Keum N, Giovannucci E: **Global burden of colorectal cancer: emerging trends, risk factors and prevention strategies.** *Nat Rev Gastroenterol Hepatol*2019, **16:**713-732.

19. Center MM, Jemal A, Smith RA, Ward E: **Worldwide variations in colorectal cancer.** *CA Cancer J Clin*2009, **59:**366-378.
20. Ye J, Zhang R, Wu F, Zhai L, Wang K, Xiao M, Xie T, Sui X: **Non-apoptotic cell death in malignant tumor cells and natural compounds.** *Cancer Lett*2018, **420:**210-227.
21. Zhang Z, Zhang Y, Xia S, Kong Q, Li S, Liu X, Junqueira C, Meza-Sosa KF, Mok TMY, Ansara J, et al: **Gasdermin E suppresses tumour growth by activating anti-tumour immunity.** *Nature*2020, **579:**415-420.
22. Wang Q, Wang Y, Ding J, Wang C, Zhou X, Gao W, Huang H, Shao F, Liu Z: **A bioorthogonal system reveals antitumour immune function of pyroptosis.** *Nature*2020, **579:**421-426.
23. Schmitt AM, Chang HY: **Long Noncoding RNAs in Cancer Pathways.** *Cancer Cell*2016, **29:**452-463.
24. Han P, Li JW, Zhang BM, Lv JC, Li YM, Gu XY, Yu ZW, Jia YH, Bai XF, Li L, et al: **The lncRNA CRNDE promotes colorectal cancer cell proliferation and chemoresistance via miR-181a-5p-mediated regulation of Wnt/β-catenin signaling.** *Mol Cancer*2017, **16:**9.
25. Carpenter S, Fitzgerald KA: **Cytokines and Long Noncoding RNAs.** *Cold Spring Harb Perspect Biol*2018, **10**.
26. Denaro N, Merlano MC, Lo Nigro C: **Long noncoding RNAs as regulators of cancer immunity.** *Mol Oncol*2019, **13:**61-73.
27. Tolba MF: **Revolutionizing the landscape of colorectal cancer treatment: The potential role of immune checkpoint inhibitors.** *Int J Cancer*2020, **147:**2996-3006.
28. Ooki A, Shinozaki E, Yamaguchi K: **Immunotherapy in Colorectal Cancer: Current and Future Strategies.** *J Anus Rectum Colon*2021, **5:**11-24.
29. Boland PM, Ma WW: **Immunotherapy for Colorectal Cancer.** *Cancers (Basel)*2017, **9**.
30. Li L, Jiang M, Qi L, Wu Y, Song D, Gan J, Li Y, Bai Y: **Pyroptosis, a new bridge to tumor immunity.** *Cancer Sci*2021, **112:**3979-3994.
31. Zhou Z, He H, Wang K, Shi X, Wang Y, Su Y, Wang Y, Li D, Liu W, Zhang Y, et al: **Granzyme A from cytotoxic lymphocytes cleaves GSDMB to trigger pyroptosis in target cells.** *Science*2020, **368**.

# Tables

Table 1

Characteristics of the COAD patients obtained from the TCGA database

| Characteristic | TCGA_COAD(n=385) |
|---|---|
| **Age(years)** | |
| =<65 | 159(41.30%) |
| >65 | 226(58.70) |
| **Gender** | |
| Male | 205(53.25%) |
| Female | 180(46.75%) |
| **Survival status** | |
| Alive | 314(81.56%) |
| Dead | 71(18.44%) |
| **Stage** | |
| Stage I | 66(17.14%) |
| Stage II | 151(39.22%) |
| Stage IIII | 103(26.75%) |
| Stage IV | 54(14.03%) |
| unknown | 11(2.86%) |
| **T classification** | |
| This | 1(0.26%) |
| T1 | 9(2.34%) |
| T2 | 68(17.66%) |
| T3 | 263(68.31%) |
| T4 | 44(11.43%) |
| **N classification** | |
| N0 | 231(60.00%) |
| N1 | 88(22.86%) |
| N2 | 66(17.14%) |
| **M classification** | |
| M0 | 286(74.28%) |

| | |
|---|---|
| M1 | 54(14.03%) |
| unknown | 45(11.69%) |

**Table 2**

**The lncRNAs identified by univariate Cox regression with pvalue<0.05**

| id | HR | HR.95L | HR.95H | pvalue |
|---|---|---|---|---|
| HOTAIR | 1.002262 | 1.000763 | 1.003763 | 0.003088 |
| LINC00402 | 1.033168 | 1.009627 | 1.057258 | 0.005525 |
| SFTA1P | 1.026793 | 1.006943 | 1.047034 | 0.00794 |
| ZRANB2-AS1 | 0.828482 | 0.709043 | 0.96804 | 0.017841 |
| LINC00461 | 1.060789 | 1.00986 | 1.114287 | 0.018733 |
| MYB-AS1 | 0.894277 | 0.807239 | 0.9907 | 0.032451 |
| DSCR8 | 1.006876 | 1.000555 | 1.013238 | 0.032954 |
| TP53TG1 | 0.998724 | 0.997509 | 0.999939 | 0.039597 |
| CYP1B1-AS1 | 1.013262 | 1.00052 | 1.026166 | 0.041305 |
| LINC00330 | 1.015966 | 1.000451 | 1.031721 | 0.043648 |
| ALMS1-IT1 | 1.006703 | 1.000045 | 1.013406 | 0.048477 |
| **HR, hazard ratio.** | | | | |

# Figures

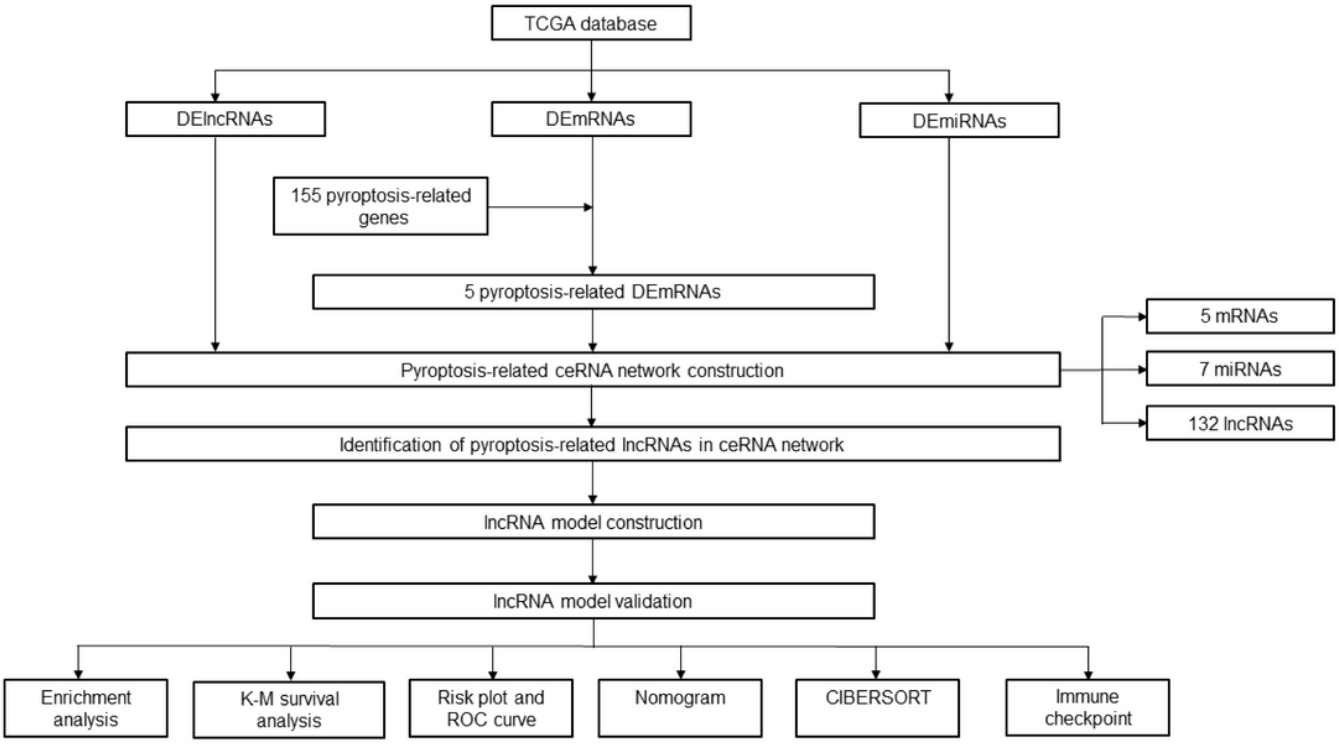


## Figure 1

The analysis process of the study. TCGA, The Cancer Genome Atlas; DElncRNAs, differentially expressed lncRNAs; DEmRNAs, differentially expressed mRNAs, DEmiRNAs, differentially expressed miRNAs; ceRNA, competitive endogenous RNA; CIBERSORT, cell-type identification by estimating relative subsets of RNA transcripts.

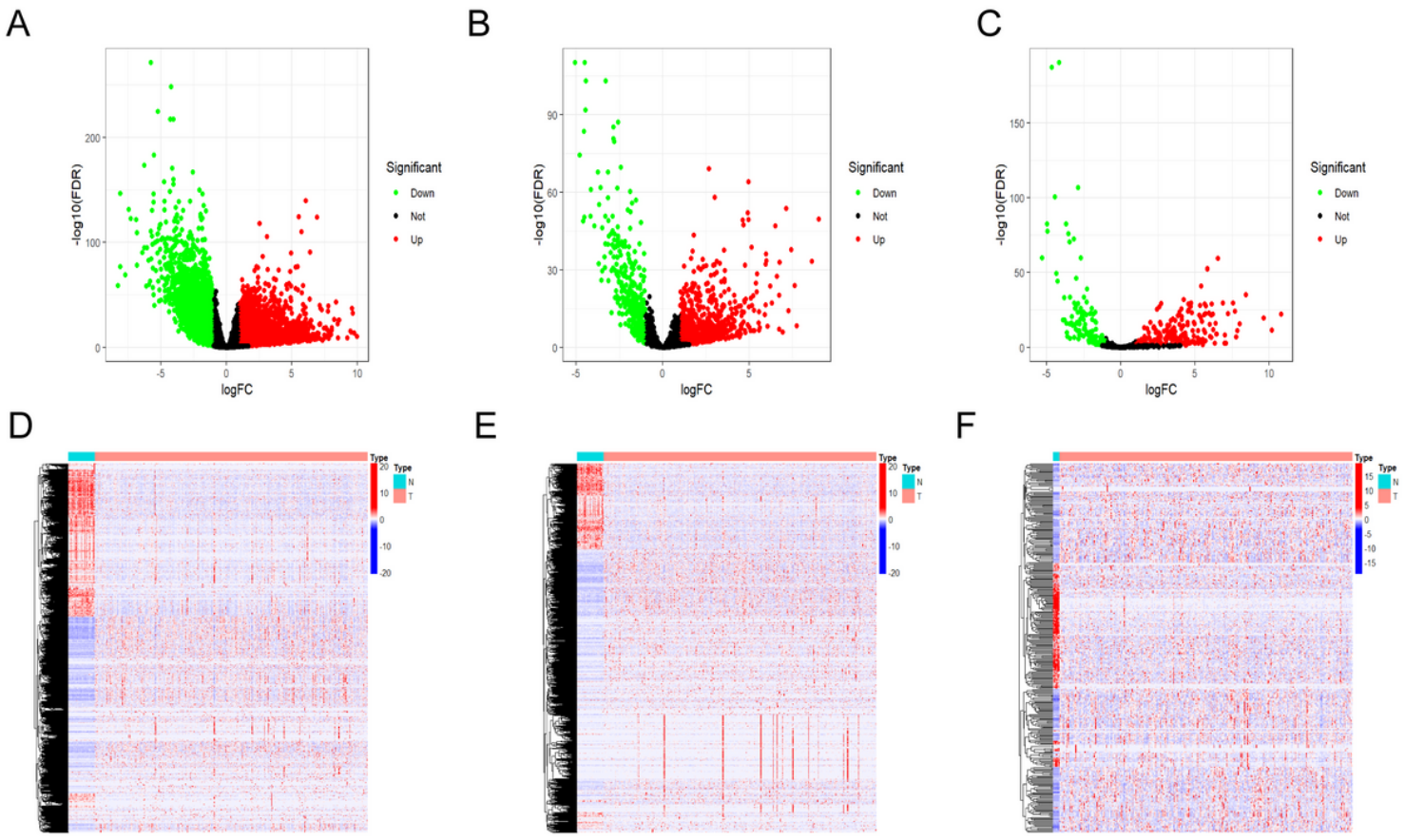


**Figure 2**

Differentially expressed genes. Volcano plots of **(A)** DEmRNAs, **(B)** DEmiRNAs and **(C)** DElncRNAs. Heatmaps of **(D)** DEmRNAs, **(E)** DEmiRNAs and **(F)** DElncRNAs.

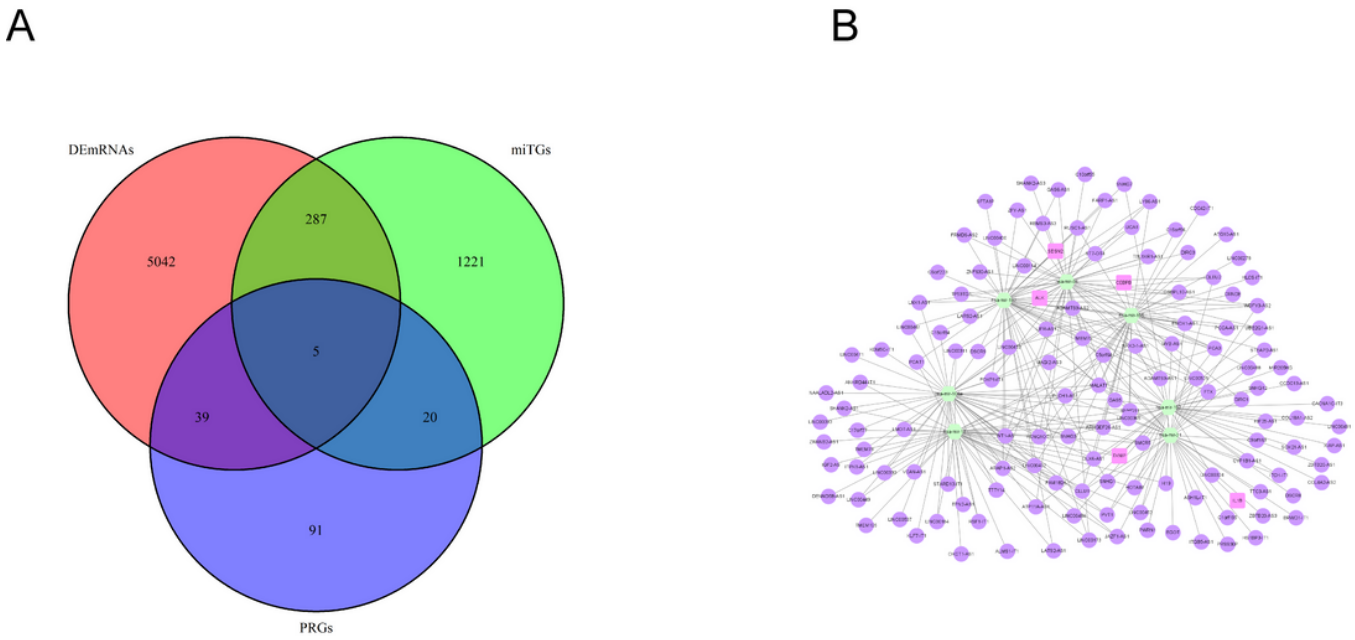

## Figure 3

The pyroptosis-related ceRNA network. **(A)** The intersection of DEmRNAs, miTGs and PRGs. **(B)** A pyroptosis-related ceRNA network. Lavender circles indicate pyroptosis-related DEmRNAs, green circles indicate DEmiRNAs and purple circles indicate DElncRNAs.

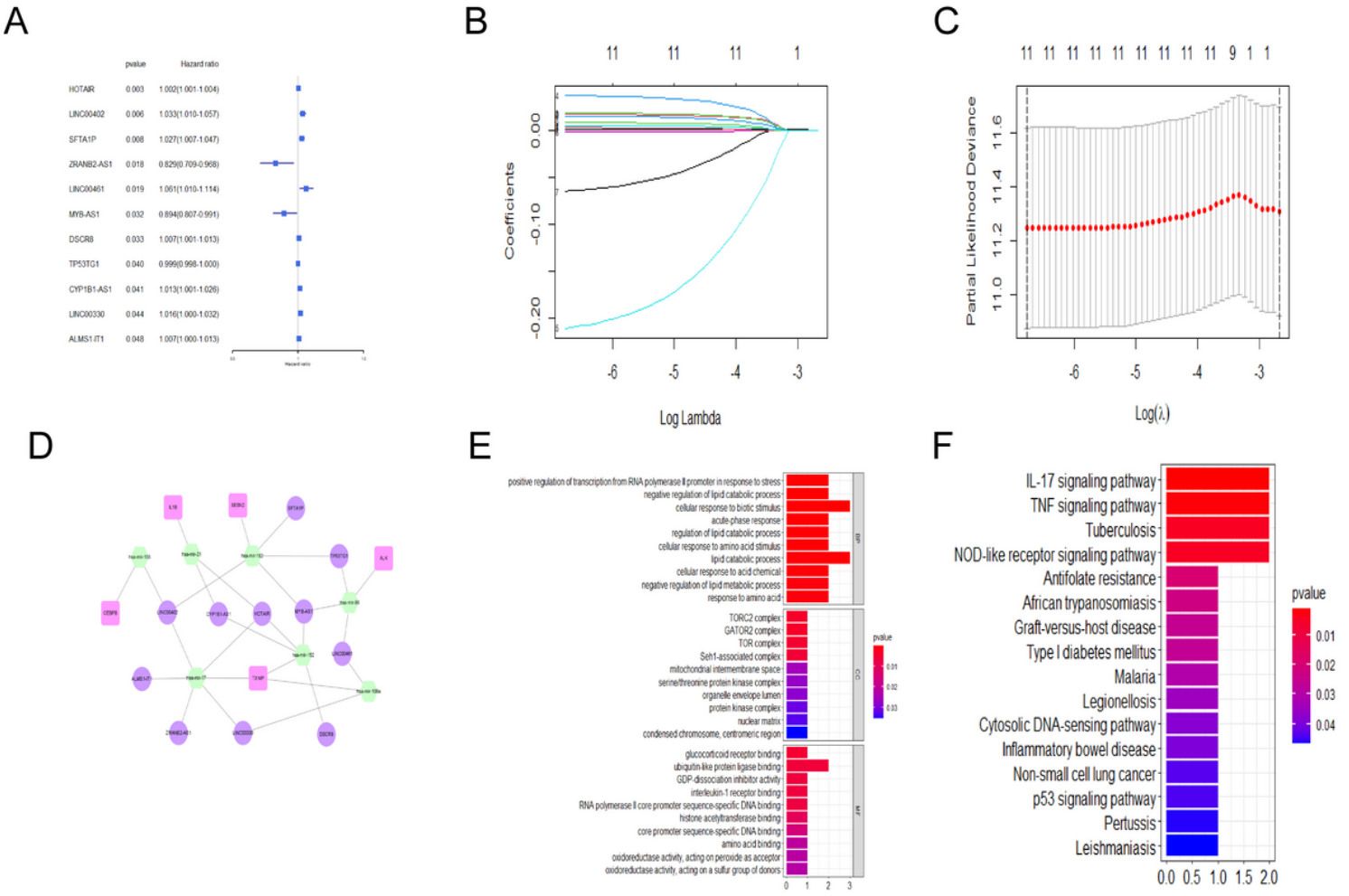


## Figure 4

The PRlncRNA risk model. **(A)** The univariate Cox regression of selected lncRNAs (Criteria: pvalue < 0.05). **(B-C)** The LASSO Cox regression analysis of lncRNAs with p<0.05. **(D)** A ceRNA network of 11 lncRNAs with 7 miRNA and 5 mRNAs based on prognostic PRlncRNA risk model. **(E-F)** GO and KEGG enrichment analysis of genes included in the above ceRNA network.

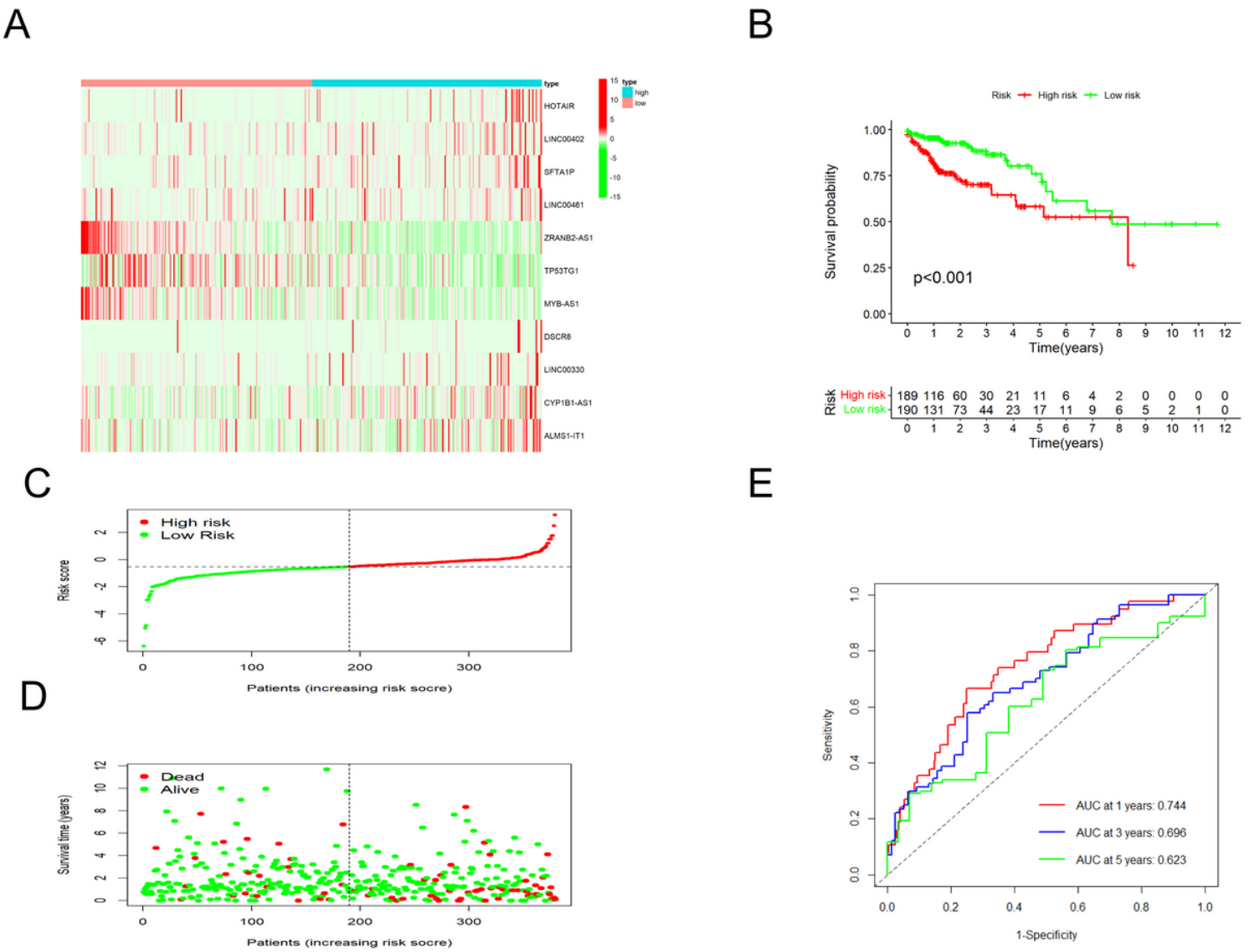


## Figure 5

Validation of the PRlncRNA risk model. **(A)** Heatmap of 11 prognostic lncRNAs between the two risk groups where red presented high expression level and green presented low expression level. **(B)** K-M analysis. **(C)** Distribution of the risk score. **(D)** The survival status of COAD patients. **(E)** ROC curves of 1-, 3-, and 5-year OS time.

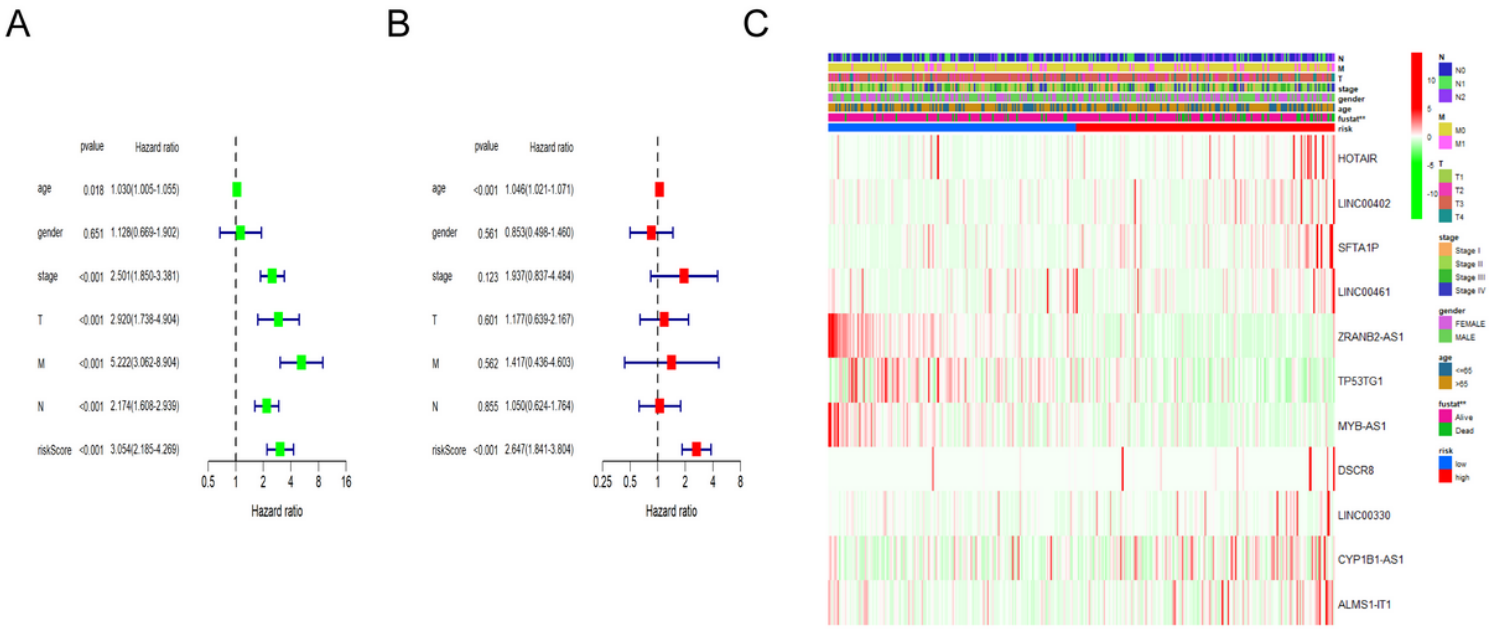


**Figure 6**

Independent prognostic analysis. **(A)** Univariate Cox analysis. **(B)** Multivariate Cox analysis. **(C)** Heatmap of the correlation of risk model and clinical characteristics (p value** < 0.01, p value* < 0.05).

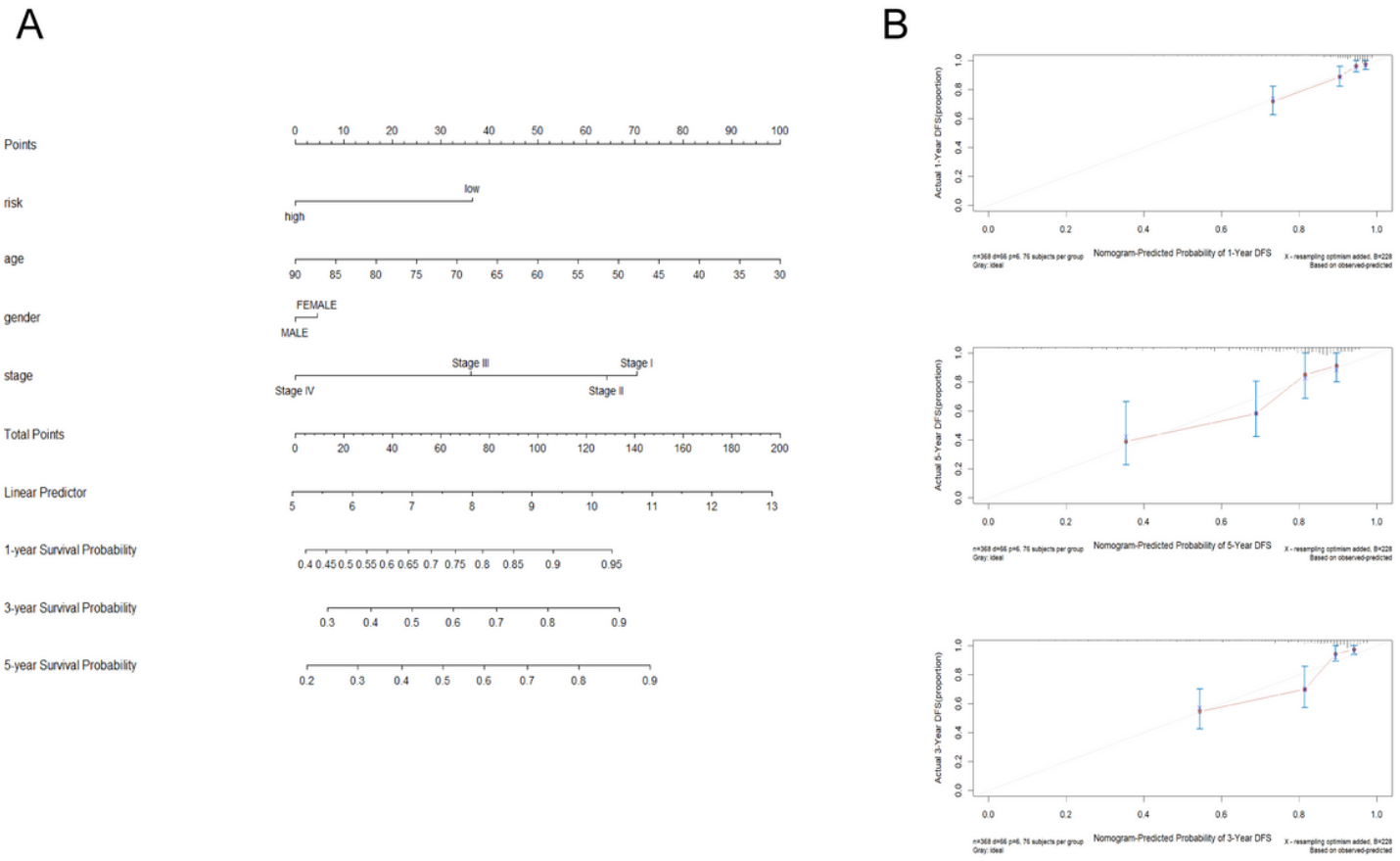


**Figure 7**

Validation of predictive ability of the risk model. **(A)** The nomogram contained risk values, age and stage to predict survival. **(B)** 1-year nomogram calibration curve. **(C)** 3-year nomogram calibration curve. **(D)** 5-year nomogram calibration curve.

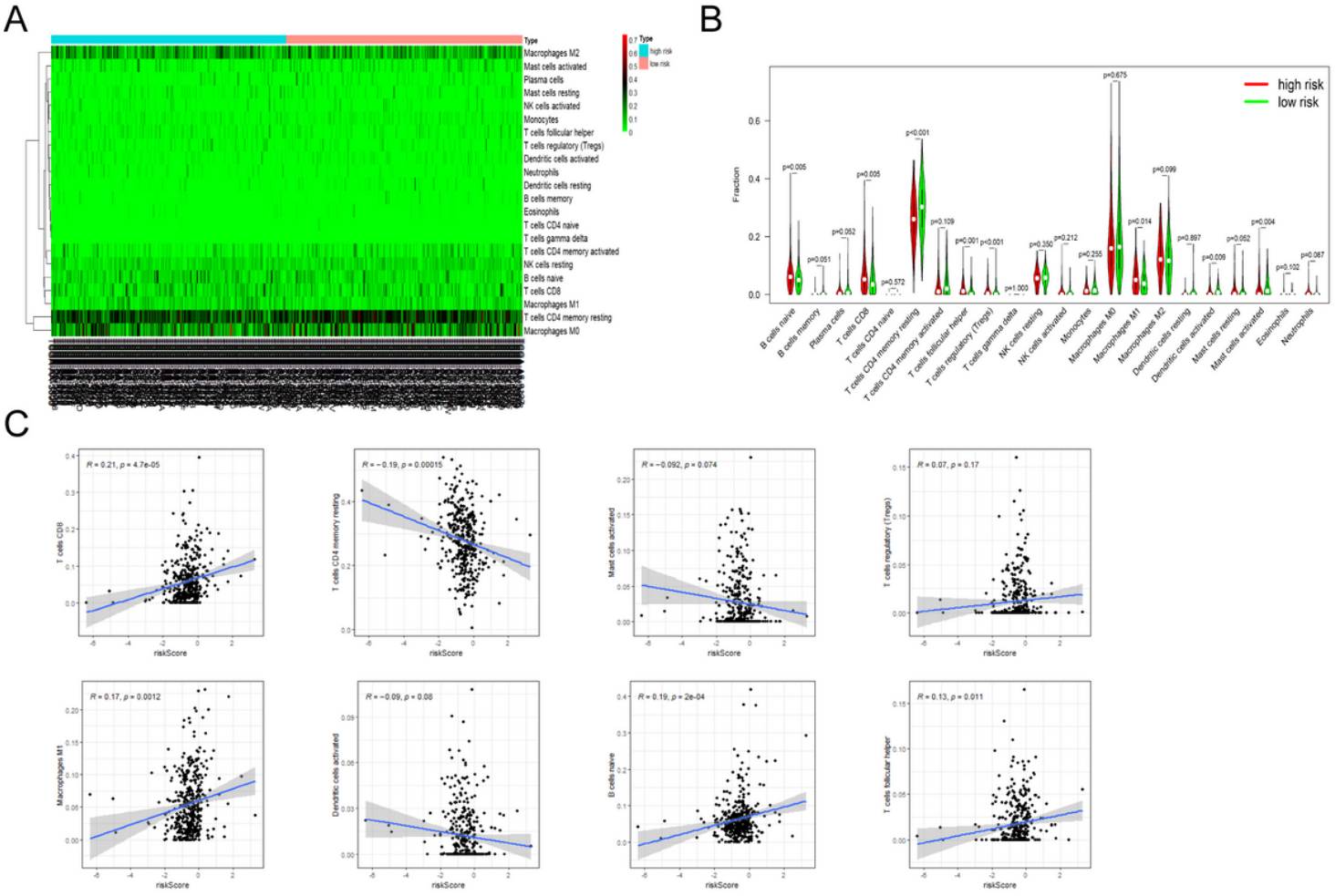


## Figure 8

Immune cell infiltration analysis. **(A)** Heatmap of the composition of the immune cells was calculated based on the CIBERSORT algorithm. **(B)** The proportion of immune cells in the two risk groups(P<0.05). **(C)** Correlation analysis between risk score and 8 immune cells (P<0.05).

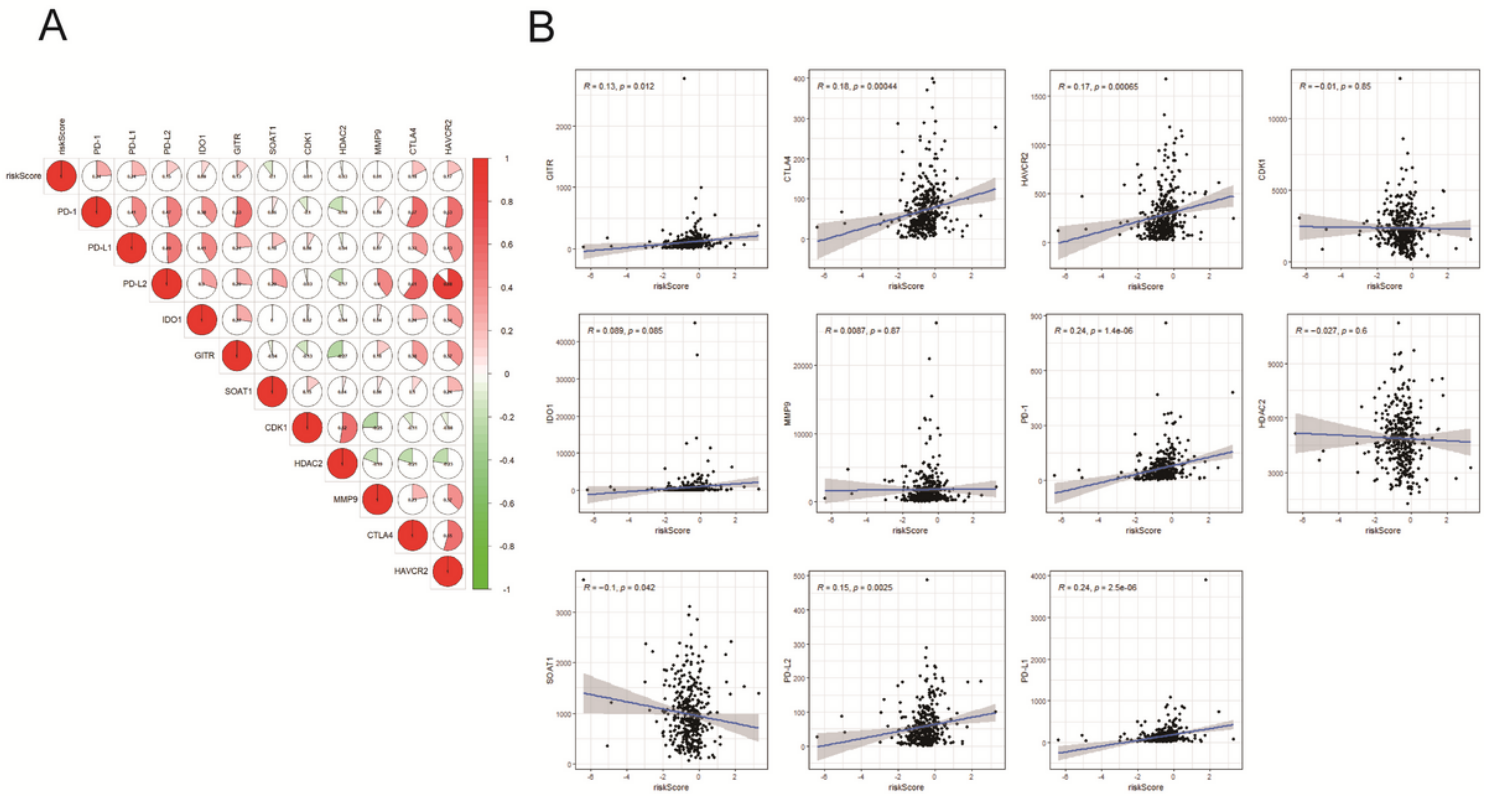


**Figure 9**

The connection between prognostic risk score and ICB-related genes. **(A)** Heatmap of the correlation of risk score and 11 ICB-related genes. **(C)** The connection between risk score and 11 ICB-related genes, respectively (P<0.05).

# Supplementary Files

This is a list of supplementary files associated with this preprint. Click to download.

- SupplementTableS1.xlsx
- SupplementTableS2.xlsx
- SupplementTableS3.xls